Title
DIFFRACTION SCATTERING AND VECTOR MESON RESONANCES

Authors
Atkinson, David
Contogouris, A.P.

Publication Date
1967-03-17

Submitted to Physical Review

UCRL-17364 c.2 rpl.
Preprint

UNIVERSITY OF CALIFORNIA

Lawrence Radiation Laboratory
Berkeley, California

AEC Contract No. W-7405-eng-48

DIFFRACTION SCATTERING AND VECTOR MESON RESONANCES

David Atkinson and A. P. Contogouris

March 17, 1967

DISCLAIMER

UCRL-17364

DIFFRACTION SCATTERING AND VECTOR MESON RESONANCES*

David Atkinson

Lawrence Radiation Laboratory
University of California
Berkeley, California

and

A. P. Contogouris†

Laboratoire de Physique Théorique et Hautes Energies,
Orsay (Seine-et-Oise), France

March 17, 1967

ABSTRACT

It is shown that, under reasonable assumptions about inelasticity and asymptotic behavior, the usual diffraction picture combined with the N/D approach to π-π scattering leads to a singular integral equation. The authors' formalism is then used to show that, in conformity with the nearby singularities philosophy, a constant left-hand discontinuity is by itself incapable of producing resonances in the GeV region. Next, a model for the

---

* This work was done under the auspices of the U. S. Atomic Energy Commission.

† Postal address: Laboratoire de Physique Théorique et Hautes Energies, Faculté des Sciences, Bât. 211, 91 - ORSAY - France.

creation of vector resonances, which combines a long-range force (defined by exchange of a cutoff vector meson) plus a short-range force (compatible with diffraction requirements), is introduced. The effect of the short-range force on the self-consistent (bootstrap) solutions is investigated in an approximate scheme. For a self-consistent solution with the correct ρ-meson mass, which is found to exist, inclusion of the short-range force is shown to decrease (by a factor of 2) the self-consistent width (which is nevertheless still greater than the experimental value).

I. INTRODUCTION

Most of the low-energy calculations on strongly interacting systems are based on the assumption that the scattering in the GeV region is determined by low-energy singularities and that the effects of the high-energy region are completely unimportant. This assumption is fully justified in pion-nucleon scattering, notably below 500 MeV, where detailed quantitative agreement between dispersion calculations and experiment has been found.[1] It is also justified in nucleon-nucleon scattering, where reasonable models account for all the important experimental features.[2]

No similar agreement can be claimed for pion-pion scattering--in particular for a self-consistent determination of the parameters of the ρ meson. For this system, it is quite possible that the effects of the high-energy region are less unimportant.[3-4] Furthermore, in a determination of the parameters of the ρ, the mass of which is rather high, the features of the amplitude in a region which starts at 2 or 3 GeV are, perhaps, of some importance.

The purpose of this work is to give a hint concerning the effect of the high-energy region on the features of the vector meson resonances. For this, the experimentally well-established picture of diffraction scattering is combined with the usual N/D approach employed in self-consistent calculations of pion-pion scattering. This leads to a marginally singular integral equation[5]

which can be solved by an application of methods developed by the authors elsewhere.[6]

In Section 2 it is shown that, under certain assumptions, both Regge behavior and the conventional diffraction picture (with nonshrinking forward peak) lead to marginally singular N/D equations. In Sec. 3 the possibility that the distant singularities (short-range forces) produce resonances in the low-energy region is studied separately. For this the basic integral equation formulated in Sec. 2 is applied to a model which consists of a constant left-hand discontinuity (and constant inelasticity). This model is compatible with the requirements of unitarity and of the diffraction picture, but completely neglects the structure of the nearby singularities; as a result it is known to be incapable of generating resonances in the GeV region. Section 4 contains the formulation of a more realistic model whose left-hand discontinuity combines a long-range part determined by vector exchange with a short-range part compatible with the requirements of diffraction scattering. Finally, in Sec. 5, the results of an approximate numerical calculation involving the model of Sec. 4 are presented and compared with the solutions of the conventional vector-meson bootstrap (without short-range part). The conclusion is that the short-range part tends to decrease significantly the coupling necessary to produce a resonance, affecting its width to a lesser extent; to reduce the self-consistent mass; and, for low cutoffs, to change

the self-consistent width in the correct direction. In particular, the width of the self-consistent solution which corresponds to $m_\rho^2 \simeq 30\, m_\pi^2$ is reduced by a factor of 2.

In Appendix A the model of Sec. 3 is reconsidered in the approximation of contracting to zero the gap between left- and right-hand cuts; this approximation has the advantage of providing explicit and relatively simple solutions. Again, it is concluded that a featureless left-hand discontinuity and inelasticity are incapable of producing acceptable resonances. Finally, the contracted-gap case, certain features of the solutions, and in particular the positions of the zeros of the denominator function, are studied in Appendix B.

II. FORMULATION OF THE BASIC EQUATIONS

Consider the elastic scattering of two pseudoscalar particles of mass unity, and assume that the partial P-wave amplitude $A_1(\nu)$ admits the usual decomposition,

$$A_1(\nu) = N(\nu)/D(\nu) \; ; \tag{2.1}$$

ν is the square of the center-of-mass momentum. It is convenient to consider once subtracted representation for N and D, with the subtraction point at $\nu = 0$. Due to the usual threshold properties, $N(0) = 0$, so the equations are

$$N(\nu) = \frac{\nu}{\pi} \int_{-\infty}^{-\omega_L} d\nu' \, \frac{\sigma(-\nu')\, D(\nu')}{\nu'(\nu' - \nu)} \; , \tag{2.2}$$

$$D(\nu) = 1 - \frac{\nu}{\pi} \int_{0}^{\infty} d\nu' \, \frac{\rho(\nu')\, R_1(\nu')\, N(\nu')}{\nu'(\nu' - \nu)} \; . \tag{2.3}$$

Here $\sigma(-\nu)$ is the discontinuity along the left-hand cut $-\infty < \nu \leq -\omega_L$, $\rho(\nu) = [\nu/\nu + 1]^{\frac{1}{2}}$ is the usual phase-space factor, and $R_1(\nu)$ is the inelasticity of the P wave;[7] thus the unitarity condition reads

$$\text{Im } A_1(\nu) = \rho(\nu)\, R_1(\nu) |A_1(\nu)|^2 \quad 0 \leq \nu < \infty \; . \tag{2.4}$$

To derive the basic integral equation of the problem, one can substitute (2.2) into (2.3). Then the definitions

$$\nu = -\omega \qquad -D(\nu)/\nu = f(\omega) \tag{2.5}$$

give

$$f(\omega) = \frac{1}{\omega} + \frac{1}{\pi} \int_{\omega_L}^{\infty} d\omega' \, K(\omega,\omega') \, \sigma(\omega') \, f(\omega') \, , \tag{2.6}$$

where

$$K(\omega,\omega') = \frac{1}{\pi} \int_0^{\infty} dx \, \frac{\rho(x) \, R_1(x)}{(x + \omega) \, (x + \omega')} \, . \tag{2.7}$$

Next, assume that, for $\nu \to + \infty$, $A_1(\nu)$ becomes purely imaginary. Equation (2.4) implies

$$\rho(\nu) \, R_1(\nu) \sim [\mathrm{Im} \, A_1(\nu)]^{-1} \, . \tag{2.8}$$

According to the Phragmen-Lindelof theorem,[8] if

$$A_1(\nu) \sim \nu^{\alpha_0}(\log \nu)^{\alpha_1}(\log\log \nu)^{\alpha_2}\cdots(\log\log\cdots\log \nu)^{\alpha_n}$$

$$\text{for } \nu \to \infty ,$$

and

$$A_1(\nu) \sim |\nu|^{\alpha_0'}(\log|\nu|)^{\alpha_1'}(\log\log|\nu|)^{\alpha_2'}\cdots(\log\log\cdots\log|\nu|)^{\alpha_n'}$$

$$\text{for } \nu \to -\infty ,$$

and if

$$|A_1(\nu)| < |ae^{(\pi - \epsilon)\nu}| , \quad \text{where } a = \text{const},$$

for all complex ν and $\epsilon > 0$, then $\alpha_0 = \alpha_0'$, $\alpha_1 = \alpha_1'$, $\cdots$, $\alpha_n = \alpha_n'$ and

$$\sigma(-\nu) \sim \text{Im } A_1(\nu) , \quad \text{for } \nu \to \infty . \tag{2.9}$$

Lest it be felt that these conditions are too restrictive, one may prefer simply to assert (2.9). Any N/D system for which Im $A_1(\nu)$ had different limits for $\nu \to \pm \infty$ would constitute a pathology lying outside the scope of this paper.

It will be shown now that all the important models of high-energy elastic scattering imply an Im $A_1(\nu)$, and hence a $\sigma(\nu)$, such that the kernel of (2.6) has an unbounded norm, so that (2.6) is a singular integral equation. For energies above a few GeV, and momentum transfers $|t|^{\frac{1}{2}} \lesssim 1$ GeV/c, a good parameterization of

the observed t-dependence of the scattering amplitude is[4]

$$|A(\nu,t)|^2 = |A(\nu,0)|^2 \; e^{tb(\nu)} \; .$$

It will be assumed that, as $\nu \to \infty$, $A(\nu,t)$ becomes purely imaginary. Then projection onto the P wave gives[9]

$$A_1(\nu) = \frac{1}{4\nu}\int_{-4\nu}^{0} dt\, A(\nu,t)\, P_1\left(1 + \frac{t}{2\nu}\right) \underset{\nu \to \infty}{\sim} i\, b^{-1}(\nu)\, \sigma_{tot}(\nu) \; ; \tag{2.10}$$

$\sigma_{tot}(\nu)$ is the total cross-section, which is taken to be asymptotically constant. As for $b(\nu)$, the width of the diffraction peak, two cases are of interest:

(i) $b(\nu) \sim \log \nu$, in accord with the hypothesis of asymptotic dominance by a Pomeranchuk Regge trajectory of non zero slope $[\alpha_P'(t = 0) \neq 0]$.

(ii) $b(\nu) \sim$ const, corresponding to the conventional diffraction picture, or to a flat Pomeranchuk trajectory.[10]

Consider first the case (i), when for $\nu \to +\infty$:

$$\text{Im}\, A_1(\nu) \sim (\log \nu)^{-1}\, \rho(\nu)\, R_1(\nu) \sim \log \nu \; . \tag{2.11}$$

The behavior of $K(\omega,\omega')$ for large ω,ω' is controlled by the

large values of the integrand in (2.7). Thus

$$K(\omega,\omega') \sim \int^{\infty} dx \, \frac{\log x}{(x+\omega)(x+\omega')} . \tag{2.12}$$

With the lower limit of integration taken at $x = 0$ this gives[11]

$$K(\omega,\omega') \sim \frac{1}{2} \, \frac{(\log \omega')^2 - (\log \omega)^2}{\omega' - \omega} . \tag{2.13}$$

In view of (2.9), $\sigma(\omega) \sim (\log \omega)^{-1}$. Thus for large ω, ω' the kernel of (2.6) reduces to

$$K(\omega,\omega') \, \sigma(\omega') \sim \frac{1}{2} \, \frac{\log \frac{\omega'}{\omega}}{\omega' - \omega} \left(1 + \frac{\log \omega}{\log \omega'}\right) . \tag{2.14}$$

The norm of this diverges (logarithmically) for large ω,ω' , so that (2.6) is a marginally singular integral equation.[12]

Consider now the case (ii). The above considerations can be easily generalized to include the asymptotic behavior $\operatorname{Re} A_1(\nu) \sim \text{const}$ together with $\operatorname{Im} A_1(\nu) \sim \text{const}$ (for $\nu \to \infty$). In view of (2.4), (2.7) can be split as follows:

$$K(\omega,\omega') = \frac{1}{\pi} \, \frac{\operatorname{Im} A_1(\infty)}{|A_1(\infty)|^2} \, \frac{\log \frac{\bar{\omega}'}{\omega}}{\omega' - \omega} + \frac{1}{\pi} \int_0^{\infty} dx \, \frac{\rho(x) \, R_1(x) - \operatorname{Im} A_1(\infty) \, |A_1(\infty)|^{-2}}{(x+\omega)(x+\omega')} . \tag{2.15}$$

Then use of (2.9) reduces (2.6) to the form

$$f(\omega) = \frac{1}{\omega} + \frac{\lambda}{\pi^2}\int_{\omega_L}^{\infty} d\omega' \, \frac{\log \frac{\omega'}{\omega}}{\omega' - \omega} f(\omega') + \frac{1}{\pi}\int_{\omega_L}^{\infty} d\omega' \, K_F(\omega,\omega') \, f(\omega') \tag{2.16}$$

where

$$\lambda \equiv \left\{ \frac{\text{Im } A_1(\infty)}{|A_1(\infty)|} \right\}^2 . \tag{2.17}$$

$K_F(\omega,\omega')$ of (2.16) contains the integral of (2.15) and the difference $\sigma(\omega)$ - Im $A_1(\infty)$. Thus, with suitable assumptions about the way $R_1(\nu)$ and Im $A_1(\nu)$ approach their asymptotic limits, the norm of $K_F(\omega,\omega')$ is finite. Then (2.16) is a standard form solved and studied in Ref. 6.[13]

Furthermore, the definition (2.17) implies

$$0 \leqslant \lambda \leqslant 1 . \tag{2.18}$$

Then it is known that solutions free of unwanted poles on the physical sheet of ν (ghost-free solutions) can be constructed by the N/D approach[6,14-16] (see also Appendix B).

The rest of this work is restricted to models of the type (ii), for which the methods developed in Ref. 6 are directly applicable.

III. INABILITY OF SHORT-RANGE FORCE TO GENERATE RESONANCES

As a first application of the foregoing formalism, consider a model with a constant left-hand discontinuity

$$\sigma(-\nu) = \text{Im } A_1(\infty) \ , \ -\infty < \nu < -\omega_L \ , \qquad (3.1)$$

and constant inelasticity

$$R_1(\nu) = R_1(\infty) = \text{Im } A_1(\infty)|A_1(\infty)|^{-2} \ ; \qquad (3.2)$$

also, the approximation $\rho(\nu) = 1$ will be made. Then, it is asked whether resonances can be produced in the GeV region. This example, which neglects basic features of the low-energy part of the amplitude, and of the long-range part of the potential, cannot be realistic for low-energy calculations. Nevertheless, it can give some idea of the relative importance of the distant singularities in the generation of the strong-interaction resonances.

Before the consideration of the main problem it will be shown that a ghost-free amplitude can be constructed by direct application of the N/D equations. Substitution of (2.3) in (2.2) gives

$$N(\nu) = B(\nu) + \frac{\nu}{\pi} R_1(\infty) \int_0^\infty d\nu' \frac{B(\nu) - B(\nu')}{\nu - \nu'} \frac{N(\nu')}{\nu'} \qquad (3.3)$$

where

$$B(\nu) = \frac{\nu}{\pi} \int_{-\infty}^{-\omega_L} d\nu' \frac{\sigma(-\nu')}{\nu'(\nu' - \nu)} \qquad (3.4)$$

or, due to (3.1):

$$B(\nu) = \frac{\text{Im } A_1(\infty)}{\pi} \log(1 + \nu/\omega_L) \, . \qquad (3.5)$$

In view of (3.2)

$$R_1(\infty) \text{ Im } A_1(\infty) \leq 1 \, ;$$

then Ref. 6 concludes that an iteration solution of (3.3) (Neumann-Liouville series expansion) exists. On the other hand, it is easy to see from (3.5) that, for any $\nu, \nu' \geq 0$,

$$B(\nu) \geq 0 \, , \quad \frac{B(\nu) - B(\nu')}{\nu - \nu'} \geq 0. \qquad (3.6)$$

Hence, all the terms in this iteration solution will be positive and

$$N(\nu) > 0, \; \nu > 0 \, . \qquad (3.7)$$

Then (2.3) implies that $-D(\nu)$ is a Herglotz function, i.e.,

$$\text{Im } D(\nu) < 0 \qquad \text{Im } \nu > 0 \tag{3.8}$$

and that

$$D(\nu) > 0 \qquad \nu < 0 \ . \tag{3.9}$$

Thus $D(\nu)$ has no zeros on the first sheet of the complex ν plane. It is concluded that the solution of Eqs. (2.2) and (2.3) which admits a Neumann-Liouville expansion will be free of ghost poles.

With (3.1), (3.2), and the approximation $\rho(\nu) = 1$, $K_F(\omega,\omega')$ of (2.16) vanishes; then, with the simplification $\omega_L = 1$ (no loss of generality), Eq. (2.16) can be written

$$\tilde{f}(\omega) = \frac{1}{\omega} + \frac{\lambda}{\pi^2} \int_1^\infty d\omega' \, \frac{\log \frac{\omega'}{\omega}}{\omega' - \omega} \, \tilde{f}(\omega') \ ; \tag{3.10}$$

λ is given by (2.17). A solution of this equation is

$$\tilde{f}(\omega) = \frac{1}{\omega} + \lambda \int_1^\infty d\omega' \, R(\omega,\omega';\lambda) \, \frac{1}{\omega'} \ , \tag{3.11}$$

where $R(\omega,\omega';\lambda)$ is a resolvent of (3.10). Reference 6 shows that there exists a unique resolvent with a branch point only at $\lambda = 1$:

$$R(\omega,\omega';\lambda) = \frac{1}{2}\int_{-\infty}^{\infty} ds\, \frac{s\tanh(\pi s)}{\cosh^2(\pi s) - \lambda} P_{-\frac{1}{2}+is}(2\omega - 1)\, P_{-\frac{1}{2}+is}(2\omega' - 1) . \tag{3.12}$$

Thus, the extra requirement of analyticity at $\lambda = 0$ (and thus the existence of a Neumann-Liouville expansion) leads to the unique choice (3.12); in the next section this choice is further supported by certain continuity arguments.

Substitution of (3.12) into (3.11) and use of the identity[17]

$$P_{-\frac{1}{2}+is}(z) = \frac{\cosh \pi s}{\pi}\int_{1}^{\infty} \frac{dx}{x + z} P_{-\frac{1}{2}+is}(x) \quad (z > -1) \tag{3.13}$$

gives the solution

$$\tilde{D}(-\omega) = \omega\tilde{f}(\omega)$$

$$= 1 + \frac{\lambda\pi\omega}{2}\int_{-\infty}^{\infty} ds\, \frac{s\tanh(\pi s)}{\cosh^2(\pi s) - \lambda} \frac{P_{-\frac{1}{2}+is}(2\omega - 1)}{\cosh(\pi s)} . \tag{3.14}$$

The foregoing conclusions on the absence of ghost zeros of this solution can be checked directly, at least for ν real and negative (according to Appendix B this is a particularly relevant region). Figure 1 presents plots of (3.14) in the interval $1 < \omega < 700$ for various values of the parameter λ, subject to the

condition (2.18); no ghost zeros of $D(-\omega)$ are indicated.

An analytic continuation of (3.14) to $\omega < 0$ will be necessary in order to look for resonances. This is best accomplished by means of the identity[17]

$$P_\ell(-z) = e^{\mp i\ell\pi} P_\ell(z) - \frac{2}{\pi} \sin(\pi\ell)\, Q_\ell(z)$$

($\pm$ according as $\operatorname{Im} z \gtrless 0$), which gives

$$\tilde{D}(\nu) = 1 - i\lambda\pi\nu \int_0^\infty ds\, \frac{s \tanh(\pi s)}{\cosh^2(\pi s) - \lambda}\, P_{-\frac{1}{2}+is}(2\nu + 1)$$

$$- \lambda\nu \int_{-\infty}^\infty ds\, \frac{s \tanh(\pi s)}{\cosh^2(\pi s) - \lambda}\, Q_{-\frac{1}{2}+is}(2\nu + 1) . \tag{3.15}$$

To simplify the first integrand, use has been made of the symmetry property[15]

$$P_{-\frac{1}{2}+is}(z) = P_{-\frac{1}{2}-is}(z) . \tag{3.16}$$

For $\nu > 0$, because of (3.16), the contribution of the second term of (3.15) is purely imaginary. Hence the condition for a resonance at $\nu = \nu_R$ is

$$\mathrm{Re}\,\tilde{D}(\nu_R) = 1 - 2\lambda\nu_R \int_0^\infty ds\, \frac{s\,\tanh(\pi s)}{\cosh^2(\pi s) - \lambda}\, \mathrm{Re}\, Q_{-\frac{1}{2}+is}(2\nu_R + 1) = 0 \,. \tag{3.17}$$

The functions $\mathrm{Re}\,\tilde{D}(\nu)$, for $\lambda = 0.25$, 0.50, 0.75, 0.95 and 1, are plotted in Fig. 2. For $0 < \nu < 50$ there are no zeros of $\mathrm{Re}\,\tilde{D}(\nu)$; with the beginning of the left-hand cut defined by two-pion exchange ($\omega_L = m_\pi^2 = 1$) this region extends up to 2 GeV. Moreover, the weak dependence of $\mathrm{Re}\,\tilde{D}(\nu)$ on ν at large ν indicates that, probably, there are no zeros at all.

For λ close to unity ($\lambda \to 1-$) the majorizations of $R(\omega,\omega';\lambda)$ given in Ref. 6 and the asymptotic properties of the Legendre functions for large argument indicate that, apart from logarithmic factors,

$$\mathrm{Im}\,\tilde{D}(\nu) \sim \nu^{\frac{1}{2}} \,, \quad \text{for} \quad \nu \to \infty \,. \tag{3.18}$$

Since a once-subtracted representation for $\tilde{D}(\nu)$ is used, this behavior is in agreement with the conclusions of Olesen and Squires.[18]

The conclusion of this section is that a constant left-hand discontinuity along with a constant inelasticity is incapable of generating strong-interaction resonances: the real part of the corresponding denominator function does not vanish at all, at least in the GeV region. This conclusion is further strengthened by the explicit solution of Appendix A (approximation $\omega_L = 0$) .

In this model, a constant left-hand discontinuity and inelasticity can be considered as an abstraction representing the effects of the high-energy region. In this sense it can be said that for the generation of the known resonances the high-energy effects are not primarily responsible; the resonances are generated by the long-range forces. This conclusion is, of course, hardly surprising. However, the model shows also that an asymptotically constant left-hand discontinuity, which is compatible with the present experimental information in the diffraction region, in no way contradicts the basic principles of dominance by nearby singularities.

On the other hand, although not primarily responsible, the short-range force may have a significant effect on certain features of the resonances. This question is taken up in the next two sections.

IV. A MODEL COMBINING LONG- AND SHORT-RANGE FORCES

The next application of the formalism of Sec. 2 is a more realistic model with a left-hand discontinuity of which the nearby part is given by the exchange of an elementary vector meson of mass m (long-range forces), and the distant part is constant (short-range force). Thus, for $-\omega_1 < \nu < -\omega_L = -m^2/4$,[19]

$$\sigma_1(-\nu, m^2) = \gamma\left(1 + \frac{m^2+4}{8\nu}\right)\left(1 + \frac{m^2}{2\nu}\right) \theta(-\nu - \tfrac{m^2}{4})\, \theta(\omega_1 + \nu) , \tag{4.1}$$

where γ is proportional to the $\pi\pi\rho$ coupling (the width $\Gamma_{\rho \to \pi\pi} \simeq 120$ MeV corresponds to $\gamma \simeq 3.8$); and for $\nu < -\omega_1$,

$$\sigma_2(-\nu) = \lambda\, \theta(-\nu - \omega_1) , \text{ with } 0 < \lambda < 1 . \tag{4.2}$$

For simplicity, elastic unitarity $[R_1(\nu) = 1]$ will be assumed, the generalization to any asymptotically constant inelasticity being straightforward.

One way to combine (4.1) and (4.2) is indicated in Fig. 3: $\sigma_1(-\nu, m^2)$ rises on the left until it reaches the value λ. Correspondingly, ω_1 is the larger zero of the equation

$$\gamma\left(1 - \frac{m^2+4}{8\omega}\right)\left(1 - \frac{m^2}{2\omega}\right) = \lambda . \tag{4.3}$$

Unfortunately, in this model, which has the advantage of not introducing additional parameters, calculations with $0 < \lambda < 1$ and $1 \leq \gamma \leq 50$ gave no indication of zeros of Re $D(\nu)$ for energies up to $\nu = 50$. It can be said that the attractive part of the potential ($\equiv$ positive part of left-hand discontinuity) is not sufficiently strong to produce physical resonances. Notice that increase of γ strengthens the repulsion rather than the attraction.[20]

Thus one is led to a combination of (4.1), (4.2) according to Fig. 4, where a sharp cutoff, Λ, is imposed on the vector meson contribution, so that

$$\omega_1 = \Lambda \left(\frac{m^2}{4} - 1\right) . \qquad (4.4)$$

It can be shown again that for all λ, $0 < \lambda < 1$, a ghost-free amplitude exists, because an iteration solution of (3.3) can be constructed; and $B(\nu)$, as defined in (3.4), has been found to satisfy (3.6), at least for $4 < m^2 < 50$, and $\Lambda \geq 10$.

The defect of this model is that it contains two free parameters, λ and Λ. In view of the smallness of the real part of the forward amplitudes observed in high-energy p-p and π-p scattering,[4] it is perhaps reasonable to assume that λ is close to unity, say $0.9 < \lambda < 1$. However, Λ remains in principle

undetermined. Still, important information may be obtained by comparing the resulting solutions with those from a model with the same $\sigma_1(-\nu, m^2)$ (i.e., the same Λ) but with $\lambda = 0$. By keeping the same long-range part one may expect to get some information about the effect of the short-range force on various features of the amplitude.

This program will be pursued in an approximate scheme defined as follows: With the left-hand discontinuity of Fig. 4, suppose that Eq. (2.16) is written in operator form,

$$f = f_o + \lambda K_S \cdot f + K_F \cdot f \ , \tag{4.5}$$

where f_0 stands for $\frac{1}{\omega}$, K_S for the singular kernel $\frac{1}{\pi^2} \frac{\log \frac{\omega'}{\omega}}{\omega' - \omega}$, etc. When the last part $(K_F \cdot f)$ is neglected, the solution of (4.5) is given in Sec. 3 and can be written

$$\tilde{f} = f_0 + \lambda R \cdot f_0 \ ; \tag{4.6}$$

R represents the resolvent (3.12). The approximate solution that will be used is

$$\hat{f} = f_0 + (\lambda K_S + K_F) \cdot \tilde{f} \ . \tag{4.7}$$

To compare this with the exact solution, note that (4.5) can be written

$$f = (1 + \lambda R)\, f_0 + (1 + \lambda R)\cdot K_F \cdot f \quad . \tag{4.8}$$

Reference 6 has shown that for $0 < \lambda < 1$, and with the resolvent (3.12), Eq. (4.8) is Fredholm; hence, for sufficiently small λ, an iteration solution exists. The first iteration gives

$$f_1 = (1 + \lambda R)\, f_0 + (1 + \lambda R)\cdot K_F \cdot \hat{f} \quad .$$

Use of the well-known identity[20]

$$K_S \cdot (1 + \lambda R) = R$$

shows that f_1 differs from $\hat{f}$ to terms of order $\lambda ||R\cdot K_F|| \Big/ ||K_F||$.

Equations (2.15) and (2.16) show that, for $\lambda \to 0$, K_F tends to a finite limit, say $K_F^{(o)}$, so that (4.5) becomes

$$f = f_0 + K_F^{(o)} \cdot f \tag{4.9}$$

(a Fredholm equation). On the other hand, since R is the resolvent analytic at $\lambda = 0$, $\lim_{\lambda \to 0} \lambda R = 0$, and (4.8) reduces again to the form (4.9).

Suppose, however, that the calculation is carried out, not with R, but with another resolvent $R^{(1)}$, which contains a multiple of the homogeneous solution corresponding to $f = f_0 + \lambda K_S \cdot f$. It can be seen [Eq. (2.11) of ref. 18] that in the limit $\lambda \to 0$, $\tilde{f} \not\to f_0$ and $\lambda R^{(1)} \not\to 0$; hence in this case (4.9) is not reproduced. Clearly, on grounds of continuity, it is desirable that the limit $\lambda \to 0$ reproduce the situation that corresponds to simple exchange of a cutoff vector meson [Eq. (4.9)].

Note that in the limit $\lambda \to 0$, with $\tilde{f} \to f_0$, the approximate solution of (4.7) tends to $\hat{f} \to f_0 + K_F^{(o)} f_0$. Clearly, this is the first iteration of (4.9), usually called the "determinantal" solution;[21] most of the numerical results of bootstrap calculations have been obtained with this type of solution.

In terms of the solution $\tilde{D}(-\omega)$ of (3.14), Eq. (4.7) can be written

$$\hat{D}(-\omega) = 1 + \frac{\omega}{\pi} \int_{\omega_L(m^2)}^{\infty} d\omega' \, \frac{K(\omega,\omega')\ \sigma(\omega', m^2)}{\omega'} \tilde{D}(-\omega') \ , \qquad (4.10)$$

where $\sigma(\omega,m^2)$ is given by (4.1), (4.2) (or Fig. 4), and

$$K(\omega,\omega') = \frac{2}{\pi(\omega - \omega')} \left\{ \left(\frac{\omega}{\omega - 1} \right)^{\frac{1}{2}} \log[\omega^{\frac{1}{2}} + (\omega - 1)^{\frac{1}{2}}] \right.$$

$$\left. - \left(\frac{\omega'}{\omega' - 1} \right)^{\frac{1}{2}} \log[\omega'^{\frac{1}{2}} + (\omega' - 1)^{\frac{1}{2}}] \right\} . \qquad (4.11)$$

Again, to determine the resonances $(\nu > 0)$ an analytic continuation to $\omega < 0$ is needed. For this, let

$$\omega = \cosh^2(i\,\frac{\pi}{2} + y) = -\sinh^2 y$$

and, for $\omega < 0$,

$$\sinh y = (-\omega)^{\frac{1}{2}}, \text{ i.e., } y = \log[(-\omega)^{\frac{1}{2}} + (-\omega + 1)^{\frac{1}{2}}] .$$

Hence

$$\left(\frac{\omega}{\omega - 1} \right)^{\frac{1}{2}} \log[\omega^{\frac{1}{2}} + (\omega - 1)^{\frac{1}{2}}] = \left(\frac{i\pi}{2} + y \right) \tanh y$$

$$= \left\{ \frac{i\pi}{2} + \log[(-\omega)^{\frac{1}{2}} + (-\omega + 1)^{\frac{1}{2}}] \right\} \left(\frac{-\omega}{1 - \omega} \right)^{\frac{1}{2}} .$$

With this, one has

$$\operatorname{Re} \hat{D}(-\omega) = 1 + \frac{\omega}{\pi} \int_{\omega_L(m^2)}^{\infty} d\omega' \, \frac{\operatorname{Re} K(\omega,\omega')\ \sigma(\omega',m^2)}{\omega'} \, \tilde{D}(-\omega') , \qquad (4.12)$$

where

$$\text{Re } K(\omega,\omega') = \frac{2}{\pi(\omega - \omega')} \left\{ \left(\frac{-\omega}{1 - \omega} \right)^{\frac{1}{2}} \log[(-\omega)^{\frac{1}{2}} + (-\omega + 1)^{\frac{1}{2}}] \right.$$
$$\left. - \left(\frac{\omega'}{\omega' - 1} \right)^{\frac{1}{2}} \log[\omega'^{\frac{1}{2}} + (\omega' - 1)^{\frac{1}{2}}] \right\} , \qquad (4.13)$$

and

$$\text{Im } \hat{D}(-\omega) = \frac{\omega}{\pi} \int_{\omega_L(m^2)}^{\infty} d\omega' \, \frac{\text{Im } K(\omega,\omega') \; \sigma(\omega',m^2)}{\omega'} \; \tilde{D}(-\omega') , \qquad (4.14)$$

where

$$\text{Im } K(\omega,\omega') = \frac{1}{\omega - \omega'} \left(\frac{-\omega}{1 - \omega} \right)^{\frac{1}{2}} . \qquad (4.15)$$

The condition, then, for a (narrow) resonance at $\nu = -\omega = \nu_R$ is $\text{Re } \hat{D}(\nu_R) = 0$, and this results in an equation of the form

$$r = r(\nu_R, m^2) . \qquad (I)$$

(I) determines the coupling necessary to produce a resonance at $\nu = \nu_R$ (input coupling). The self-consistent (bootstrap) solutions are defined by the condition

$$m^2 = 4(\nu_R + 1) \qquad (I')$$

and by the relation of the width of the produced resonance (output width) to the coupling of the exchanged vector-meson, which is

$$\gamma = 6\pi \frac{(1+\nu)^{1/2}}{\nu^{3/2}} \left(\frac{\mathrm{Im}\, \hat{D}(\nu)}{\frac{d}{d\nu} \mathrm{Re}\, \hat{D}(\nu)} \right)_{\nu = \nu_R} . \qquad (II)$$

V. NUMERICAL RESULTS AND DISCUSSION

Numerical calculations of the program of Sec. 4 have been carried out for several cutoff values in the range $5 \leq \Lambda \leq 80$. For each Λ, two cases were compared:

(a) $\lambda = 0$ (i.e., without short-range force).

(b) $\lambda = 0.95$ (i.e., with short-range force).

In Fig. 5, four curves are shown between γ, the coupling, and ν_R/m_π^2, the resonance position, for the cutoff $\Lambda = 10$. Curve (Ia) is a plot of Eq. (I), subject to Eq. (I'), that is to say, the relation between the input, or cross-channel coupling, γ, and the mass of the produced resonance, this latter being constrained to be the same as the mass of the input resonance. Curve (Ib) is a similar plot, but this time with the short-range force added. Curve (IIa) is a plot of Eq. (II), so that γ is now the (reduced) width of the output resonance, ν_R/m_π^2 being, as before, the self-consistent resonance position. Curve (IIb) repeats this with the short-range force added. Finally, Fig. 6 is a similar graph for the cutoff $\Lambda = 40$; for other values of Λ the results remain qualitatively unchanged.

Several observations can be made within this approximate model, on the basis of Figs. 5 and 6:

(iii) In general, bootstrap solutions exist both without the short-range force (intersection of curves Ia and IIa) and

with the short-range force (intersection of Ib and IIb).

For each case (a), (b), the self-consistent mass and width as a function of Λ is presented in Fig. 7. For all Λ the addition of the short-range force decreases the self-consistent mass. For large Λ, the differences $\gamma_{(a)} - \gamma_{(b)}$ and $(m_\rho/m_\pi)^2_{(a)} - (m_\rho/m_\pi)^2_{(b)}$ are small, as they should be (most of the left-hand discontinuity being given by the ρ-exchange); but as Λ decreases, these differences increase.

It is of particular interest that a bootstrap solution with the correct ρ-meson mass $(m_\rho^2 = 30)$ does exist. Here the short-range attraction decreases the self-consistent width by a factor of 2 (from $\gamma_{(a)} \simeq 48$ to $\gamma_{(b)} \simeq 22$).

However, even with a short-range force, this width remains about six times as large as the experimental value. Thus, the conclusion is that the addition of the short-range attraction acts in the correct direction, but is not sufficient to explain the whole magnitude of the discrepancy.

(i) For a given resonance position ν_R/m_π^2, the addition of the short-range force decreases significantly the necessary input coupling γ (cf. curves Ia and Ib). This is true for each cutoff, and is an eminently reasonable state of affairs: if a short-range attraction is present, the long-range force needed to produce a resonance at a given

position is reduced. Similarly, for a given γ, the resonance mass is decreased by the addition of the long-range force.

(ii) For a given ν_R, the short-range force increases the width of the output resonance, however (cf. curves IIa and IIb). This is not surprising, for it is known that what is required to narrow the output resonance, for a given mass, is the addition of a long-range repulsion,[22] rather than a short-range attraction.

Of course, in this calculation many important contributions to the binding force have been omitted. For example, the exchange of two pions in relative S state could be significant, either if its contribution is strongly repulsive,[22] or if it is strongly attractive, with perhaps a resonance.[23] It is even possible that multi-particle exchange is important. Moreover, this simple model has neglected inelasticity. It is possible that a one-channel calculation would require a CDD pole, even if the correct inelasticity were used,[24] and that a dynamical calculation could only be done with good accuracy in a many-channel scheme. An SU(3) model in which the $K\bar{K}$ channel was also incorporated suggested that this channel might not be too important;[25] but an SU(6) model, in which the $\pi\omega$ channel also occurs, would, if it is to be believed, require a one-channel CDD pole, or equivalently

a many-channel ND^{-1} system.[26] In this connection, it is interesting that a calculation by Fulco, Shaw, and Wong[27] of the ρ meson in the three-channel system $(\pi\pi, K\bar{K}, \pi\omega)$ with a cutoff, and no short-range force, gives, as usual, a resonance width that is too large, although the $K\bar{K}$ and $\pi\omega$ channels do assist in reducing the ρ-width. It can be expected that the direction and order of magnitude of the effect of a short-range force will be the same in a more sophisticated model of this kind as it was in the work presented here. That is, we may expect a singular tail to assist materially in the narrowing of the $\pi\pi$ P-wave resonance.

From the mathematical point of view the fact that the numerical calculations were done in an approximate scheme may be considered as unsatisfactory. It would certainly be of interest to repeat the whole program with the exact solution of (2.16) [or (4.5)]; and in view of the presented formalism and of the methods developed in Ref. 6, which reduce the singular to a Fredholm equation, this can be done in a straightforward manner.

ACKNOWLEDGMENTS

This work was started while the authors were at CERN, Geneva. One of them (D.A.) is indebted to Prof. R. J. Eden for discussions. The other (A.P.C.) is grateful to Dr. V. Müller for helpful conversations and criticism, to Drs. J. D. Bessis, B. Diu and A. Martin for discussions, and to Prof. Ph. Meyer for the hospitality extended to him at Orsay. Finally, the authors are deeply indebted to Mr. G. Sheppey for performing the numerical calculations; for these the CERN CDC 6600 computer was used.

APPENDIX A

In this Appendix Eq. (3.10) is solved under the assumptions (3.1), (3.2), plus the additional approximation involved in eliminating the gap between the left- and right-hand cuts ($\omega_L = 0$). This simplification, along with (3.1) and (3.2), can be characterized as a high-energy approximation. Such a situation is even more unrealistic than that of Sec. 3; however, insofar as one is concerned with the effects of the distant parts of the discontinuities on the resonance region, and because of the possibility of obtaining explicit and relatively simple solutions, its study is, perhaps, of some interest.

A disadvantage of this treatment is that, by replacing $\omega_L = 1$ by $\omega_L = 0$, the mass scale has been lost. Thus, it is necessary to subtract the N and D equations at some point $\nu = \nu_0 = -\omega_0$ (not the normal threshold), at which $D(\nu)$ can be normalized to unity; the value of ω_0 reintroduces a mass-scale. With

$$R_1(\infty)\, N(-\omega_0) = a\,, \tag{A.1}$$

the integral equation becomes

$$f(\omega) = \frac{1}{\omega - \omega_0} + \frac{a}{\pi}\,\frac{\log(\omega/\omega_0)}{\omega - \omega_0} + \frac{\lambda}{\pi^2}\int_0^\infty d\omega'\,\frac{\log(\omega'/\omega)}{\omega' - \omega}\,f(\omega')\,. \tag{A.2}$$

In operator notation this can be written

$$f = a_1 + a_2 + \frac{\lambda}{\pi^2} Kf \ , \qquad (A.3)$$

where

$$a_1 \Longrightarrow \frac{1}{\omega - \omega_0} \qquad a_2 \Longrightarrow \frac{a}{\pi} \frac{\log(\omega/\omega_0)}{\omega - \omega_0} \qquad K \Longrightarrow \frac{\log(\omega'/\omega)}{\omega' - \omega} \ .$$

Then, defining f_1, f_2 by

$$f_i = a_i + \frac{\lambda}{\pi^2} Kf_i \quad \text{for} \quad i = 1, 2, \qquad (A.4)$$

one has

$$f = f_1 + f_2 \ . \qquad (A.5)$$

The functions f_i are solutions of (A.4), which can be expressed in the form

$$f_i = a_i + \lambda R a_i \ , \qquad (A.6)$$

where R is a resolvent of the kernel $\frac{1}{\pi^2} K$, satisfying

$$R = \frac{1}{\pi^2} K + \frac{\lambda}{\pi^2} K \cdot R \ . \qquad (A.7)$$

It was shown in Ref. 6 that R exists but is not unique; it has a two-parameter manifold. However, if the solution is required to have no singularity at $\lambda = 0$, and thus to admit a perturbation expansion in powers of λ, a unique resolvent is singled out, which has a branch point only at $\lambda = 1$ (see also Appendix B). This resolvent is

$$R(\omega,\omega';\lambda) = \frac{1}{\pi[\lambda(1 - \lambda)]^{\frac{1}{2}}} \frac{\sinh [S_0 \log(\omega'/\omega)]}{\omega' - \omega} , \tag{A.8}$$

where

$$\lambda = \sin^2(\pi S_0) \quad S_0 = \frac{1}{i\pi} \log[(-\lambda)^{\frac{1}{2}} + (1 - \lambda)^{\frac{1}{2}}] ,$$

with $0 < S_0 < \frac{1}{2}$ for $0 < \lambda < 1$.

One might solve the two equations (A.4) by using the resolvent (A.8). To find $f_1(\omega)$ it is necessary to evaluate (A.6) for $i = 1$ by performing the integral explicitly. The result is

$$f_1(\omega) = \frac{1}{\omega - \omega_0} \cosh[S_0 \log(\omega/\omega_0)] . \tag{A.9}$$

The equation for $f_2(\omega)$ is trivial, since

$$a_2(\omega) = \frac{a}{\pi} K(\omega,\omega_0) , \tag{A.10}$$

so that by comparing (A.4) for $i = 2$ with (A.7) one has immediately

$$f_2(\omega) = a\pi\, R(\omega,\omega_0;\lambda) . \qquad (A.11)$$

Finally, by (A.5), one has the solution

$$\begin{aligned} D(\nu) &= (\omega - \omega_0)\, f(\omega) \\ &= \cosh[S_0 \log(\omega/\omega_0)] + \frac{1}{B} \sinh[S_0 \log(\omega/\omega_0)] , \end{aligned} \qquad (A.12)$$

where

$$B \equiv \frac{[\lambda(1-\lambda)]^{\frac{1}{2}}}{a} .$$

Substituting $\omega = -\nu$, one has, for ν real and positive ($\equiv$ physical region), the following real and imaginary parts:

$$\begin{aligned} \text{Re } D(\nu) &= \cos(\pi S_0)\, [\cosh(S_0 \log \frac{\nu}{\omega_0}) + \frac{1}{B} \sinh(S_0 \log \frac{\nu}{\omega_0})] , \\ \text{Im } D(\nu) &= \sin(\pi S_0)\, [\sinh(S_0 \log \frac{\nu}{\omega_0}) + \frac{1}{B} \cosh(S_0 \log \frac{\nu}{\omega_0})] . \end{aligned} \qquad (A.13)$$

Now, the condition for a resonance at $\nu = \nu_R$ is Re $D(\nu_R) = 0$, i.e.,

$$\tanh(S_0 \log(\nu_R/\omega_0)) = -B . \qquad (A.14)$$

As ν_R changes from zero to infinity the left-hand side progresses monotonically from -1 to +1. Accordingly, if $|B| < 1$ there is one, and only one solution of (A.14), while if $|B| > 1$ there are no solutions. In the former case the coupling (or, equivalently, the width) of the resonance is

$$\frac{g^2}{4\pi} \simeq \frac{3}{\nu_0} \left[\frac{\text{Im } D(\nu)}{\frac{d}{d\nu} \text{Re } D(\nu)} \right]_{\nu = \nu_0}$$

$$= \frac{3}{S_0} \tan(\pi S_0) = \left(\frac{\lambda}{1 - \lambda} \right)^{\frac{1}{2}} \frac{3\pi}{\text{arc sin } \lambda^{\frac{1}{2}}} . \qquad \text{(A.15)}$$

In the first equality of (A.15) the phase-space factor $\left(\frac{\nu_0 + 1}{\nu_0} \right)^{\frac{1}{2}}$ has been replaced by unity. Notice that the subtraction point, ω_0, and the subtraction constant, $N(-\omega_0)$, (or equivalently B) have disappeared, and (A.15) is a simple equation involving only λ and the width $g^2/4\pi$.

Hence, in the approximation $\omega_L = 0$, and provided that $|B| < 1$, a constant l.h. discontinuity is capable of producing a resonance at some point $\nu = \nu_R$ satisfying (A.14). However, one can see from (A.15) that for all λ, $0 < \lambda < 1$, the corresponding width is exceedingly large ($g^2/4\pi > 3\pi$; compare, for example, with the experimental value for the width of $\rho \to 2\pi$: $g_{\rho\pi\pi}^2/4\pi \simeq 0.6$). Such a wide resonance can hardly produce any of the usual effects on the cross-section of the corresponding process (and hardly justifies

the use of formulas like (A.15), which are meaningful only for narrow resonances). Thus it cannot be considered acceptable.

To find solutions of the equation

$$\frac{g^2}{4\pi} = \frac{3}{s_0} \tan(\pi s_0)$$

corresponding to $g^2/4\pi \simeq 1$ one needs s_0 outside the interval $0 < s_0 < \frac{1}{2}$. As the first Riemann sheet of the λ-plane corresponds to $-\frac{1}{2} < s_0 < \frac{1}{2}$ this means that one has to go to higher λ-sheets. On the higher sheets branch points exist at both $\lambda = 0$ and $\lambda = 1$ (see Appendix B); moreover, the continuation of a solution onto a higher sheet is not necessarily a solution of the original equation, because the integral in (A.2) will no longer converge. The continued solution corresponds to a higher CDD class.[14] Thus, in fine, there is no resonance with acceptable width generated by a featureless, constant left-hand discontinuity.

APPENDIX B

The purpose of this Appendix is twofold: First, to present the sheet structure in λ of the resolvent of Appendix A [Eq. (A.8)]; second, to study in certain simple examples (corresponding to $\omega_L = 0$) the zeros of the denominator function. As the approximation $\omega_L = 0$ leads to relatively simple explicit solutions having a number of features in common with the exact ones, the conclusions are expected to provide useful insight.

To find the structure of (A.8) it is convenient to map the infinity of Riemann sheets in λ onto the complex plane of another appropriate variable w defined by

$$\lambda = \cos^2(\pi w). \tag{B.1}$$

Under this mapping,

$$R(\omega,\omega';\lambda) = \frac{2}{\pi(\omega - \omega')} \frac{\sinh\left[\left(\frac{1}{2} - w\right) \log \frac{\omega'}{\omega}\right]}{\sin(2\pi w)} . \tag{B.2}$$

This is a meromorphic function of w; its poles correspond to branch points in λ and appear at

$$w = m , \quad m = 0, \pm\tfrac{1}{2}, \pm 1, \pm\tfrac{3}{2}, \cdots . \tag{B.3}$$

Thus, the various sheets of λ are mapped onto parallel strips of the w-plane (Fig. 8).

The point $\lambda = 0$ corresponds to $m = \pm \frac{1}{2}, \pm \frac{3}{2}, \cdots$. In particular $w = \frac{1}{2}$ does not lead to a singularity of (B.2); and as the first sheet of λ corresponds to $0 < \mathrm{Re}\ w < 1$ it is concluded that (B.2) has no singularity at $\lambda = 0$ on the first sheet. However, on higher sheets $\lambda = 0$ is a branch point.

Sheet II is defined to be the sheet connected to sheet I across the cut $1 \leq \lambda < \infty$ and maps onto the strip $1 < \mathrm{Re}\ w < \frac{3}{2}$. Here there are branch points at both $\lambda = 0$ (cut $-\infty < \lambda < 0$) and $\lambda = 1$ (cut $1 < \lambda < \infty$), and this is true for all higher sheets. It follows that a double circuit around $\lambda = 1$ which does not enclose $\lambda = 0$ (C_1 of Fig. 8) brings one back onto sheet I; however, circuits enclosing $\lambda = 0$ and $\lambda = 1$ (C_2 of Fig. 8) lead into higher sheets. Notice the similarities with the sheet-structure of the exact resolvent (for $\omega_L \neq 0$):[15] as in that case, the branch points may be said to behave individually like square roots but together like a logarithm.

Consider now the zeros of $D(\nu)$ corresponding to the resolvent (B.2), and take (for simplicity) $N(-\omega_0) = 0$. Then Eq. (A.12) reduces to

$$D(-\omega) = \cosh\left(S_0 \log \frac{\omega}{\omega_0}\right) . \qquad \text{(B.4)}$$

Clearly, the physical sheet of ω is

$$-\pi < \arg \omega < \pi \tag{B.5}$$

and corresponds to $0 < \arg \nu < 2\pi$.

Suppose now that λ varies over real values. At first $-\infty < \lambda < 0$ corresponds to $w = k + \frac{1}{2} + iv$, $k = 0, \pm 1, \pm 2, \cdots$, and $0 < v < \infty$ (or $-\infty < v < 0$). Hence $\lambda = -\sinh^2(\pi v)$, $S_0 = -iv$, and the zeros of (B.4) appear at

$$\omega = \omega_0 \exp[n + \tfrac{1}{2}) \tfrac{\pi}{v}] \quad n = 0, \pm 1, \pm 2, \cdots . \tag{B.6}$$

This gives two sets, each of an infinite number of zeros lying on the positive real ω-axis; for $0 < v < \infty$, the one set, which corresponds to $n = -1, -2, -3, \cdots$, accumulates at $\omega = 0$, and the other set ($n = 0, 1, 2, \cdots$) accumulates at $\omega = \infty$. In view of (B.5) these zeros lie on the physical sheet of the complex ν-plane (along the negative real ν-axis).

Next, suppose that λ varies on its first sheet along $0 < \lambda < 1$. From Fig. 8 this corresponds to w = real, $0 < w < 1$. Now, the zeros of (B.4) appear at

$$\omega = \omega_0 \exp\left[\frac{(2n + 1)\,\pi}{2w - 1}\right] \quad n = 0, \pm 1, \pm 2, \cdots .$$

For all n, and w in $0 < w < 1$,

$$|\arg \omega| > \pi \ .$$

Hence, none of these zeros lies on the physical sheet of ω (or ν).

Finally, let $\lambda > 1$. This corresponds to $w = k + iv$, $k = 0, \pm 1, \pm 2, \cdots$, and $0 < \nu < \infty$ (or $-\infty < \nu < 0$). Hence $\lambda = \cosh^2(\pi v)$ and the zeros of (B.4) appear at

$$\omega = \omega_0 \exp\left[(2n + 1)\,\pi\,\frac{2v - i}{(2v)^2 + 1}\right] \qquad n = 0, \pm 1, \pm 2, \cdots .$$

For all v, $0 < v < \infty$, this relation gives at least one pair of complex zeros on the physical sheet of ω. Note that the zeros of each pair do <u>not</u> appear at complex conjugate positions; in this case the Riemann-Schwartz reflection symmetry is violated.

The conclusion is that for $\lambda < 0$ and $\lambda > 1$ the denominator function has zeros on the physical sheet of the complex ν-plane which correspond to unwanted poles of the amplitude (ghosts). However, for $0 < \lambda < 1$ these zeros disappear from the physical sheet.

This conclusion can be further strengthened by similar analysis of a different resolvent. E.g.,

$$R^{(1)}(\omega,\omega';\lambda) = \frac{1}{2\pi\,(\lambda(\lambda - 1))^{\frac{1}{2}}}\,\frac{\sin\left(q_0 \log \frac{\omega'}{\omega}\right)}{\omega' - \omega}\,\frac{\omega' + \omega}{(\omega'\omega)^{\frac{1}{2}}} \ ,$$

where

$$q_0 = \frac{1}{\pi} \log[\lambda^{\frac{1}{2}} + (\lambda - 1)^{\frac{1}{2}}]$$

is one of the resolvents of (A.2) having a branch point at $\lambda = 0$.[6] Here, for $-\infty < \lambda < 0$, $D(\nu)$ has at least one complex pair of zeros on the first sheet of ν (violating the Riemann-Schwarz symmetry); and for $\lambda > 1$ it has a double infinity of zeros along $-\infty < \nu < 0$. However, again for $0 < \lambda < 1$, no zeros appear on the physical sheet of ν.

In view of these examples and of more general theorems on the existence of ghost-free solutions of partial-wave dispersion relations,[16] one presumes that only the case $0 < \lambda < 1$ (considered in Secs. 2-5) can possibly lead to solutions of physical interest.

FOOTNOTES AND REFERENCES

1. J. Hamilton, "Dynamics of the π-N System", V. Int. Universitatswochen für Kernphysik, Schladming (1966).

2. A. Scotti and D. Y. Wong, Phys. Rev. 138, B145 (1965); H. G. Dosch and V. F. Müller, Nuovo Cimento 39, 886 (1965).

3. H. Burkhardt, Nuovo Cimento 42, 351 (1966).

4. L. Van Hove, "Theoretical Problems in Strong Interactions at High Energies", CERN 65-22 (1965).

5. That in pion-pion scattering the usual diffraction requirements lead to a singular integral equation has independently been concluded by D. H. Lyth, "Consequences of Pure Absorption at High Energies for the Prediction of Partial Waves from Unitarity", University of Birmingham preprint.

6. D. Atkinson and A. P. Contogouris, Nuovo Cimento 39, 1082 (1965).

7. G. F. Chew and S. Mandelstam, Phys. Rev. 119, 467 (1960).

8. E. C. Titchmarsh, "The Theory of Functions", Oxford University Press (1960).

9. In deriving (2.10) is is assumed that the contribution to the integral from large $|t|$ can be neglected.

10. See e.g., L. Van Hove, Rapporteur's Report at XIIIth International Conference on High Energy Physics at Berkeley, CERN Th. 714, and M. Gell-Mann, "Current Topics in Particle Physics", Cal-Tech preprint (1966).

11. Gradstein-Ryshik, "Tables of Integrals, Sums, etc.", Moscow (1963), p. 547.

12. Note that in (2.14) the first paper of the kernel $\left(\frac{1}{2}\,\frac{\log\frac{\omega'}{\omega}}{\omega'-\omega}\right)$ has

been treated in ref. 6; and the second part leads to a singular equation which is reduced to the forms of ref. 6 by a simple change of the unknown function ($f(\omega) \to \log\omega \cdot f(\omega)$).

13. Other possibilities, e.g., $b(\nu) \sim \nu^{-\frac{1}{2}}$, lead also to marginally singular integral equations of the type treated in ref. 6.

14. D. Atkinson and D. Morgan, Nuovo Cimento 41, 559 (1966).

15. D. Atkinson, J. Math. Physics, 7, 1607 (1966).

16. A. P. Contogouris and A. Martin: Existence of Solutions of Partial Wave Dispersion Relations and Singular N/D Equations, CERN preprint (1966).

17. A. Erdelyi (Ed.): Higher Transcendental Functions, Vol. 2, (New York, 1953).

18. P. Olesen and E. J. Squires, Nuovo Cimento 39, 956 (1965).

19. A. P. Contogouris and D. Atkinson, Nuovo Cimento 39, 1102 (1965).

20. The particular case $\gamma = \lambda(\omega_1 = \infty)$ corresponds to a left-hand discontinuity given entirely by exchange of an elementary vector meson. Here, for $0 < \gamma < 1$ no zeros of Re $D(\nu)$ are indicated in the region $\nu \lesssim 50$. For $\gamma > 1$ A. Bassetto and F. Paccanoni, Nuovo Cimento 44A, 1139 (1966), report the existence of a bootstrap solution free of arbitrary parameters, which in fact gives both the width and mass of the ρ in very good agreement with experiment. However, as has been stressed by those authors, the corresponding D-function is expected to have unwanted zeros.

21. F. Smithies, "Integral Equations", Cambridge University Press (1962).

22. F. Zachariasen, Scottish Universities' Summer School Lecture Notes, Edinburgh (1964).

23. G. F. Chew, Phys. Rev. 140, B1427 (1965).

24. "New Evidence for the Sigma Meson", C. Lovelace, R. M. Heinz, A. Donnachie, CERN preprint Th. 681.

25. E. J. Squires, Nuovo Cimento 34, 1751 (1964).

26. D. Atkinson, K. Dietz, D. Morgan, Ann. Phys. 37, 77 (1966).

27. "Possible One-Channel CDD Poles in πN and $\pi\pi$ Scattering", D. Atkinson and M. B. Halpern, Phys. Rev. 150, 1377 (1966).

28. J. R. Fulco, G. L. Shaw, D. Y. Wong, Phys. Rev. 137, B1242 (1965).

FIGURE CAPTIONS

Fig. 1. The function $\tilde{D}(\nu)$, given by Eq. (3.14), for real negative ν.

Fig. 2. The function Re $\tilde{D}(\nu)$, given by Eq. (3.17), for real positive ν.

Fig. 3. One possible way to combine long- and short-range forces; however, the attraction is insufficient to generate resonances at $\nu \leq 50$.

Fig. 4. Left-hand discontinuity in a realistic model combining long- and short-range forces.

Fig. 5. Bootstrap solutions in the model of Fig. 4 for a cutoff $\Lambda = 10$. The curves I represent Eq. (I) of Sec. 4 subject to the condition (I'); the curves II represent Eq. (II). The case (a) corresponds to absence of short-range force; the case (b) to presence of short-range force.

Fig. 6. The same as in Fig. 5 for $\Lambda = 40$.

Fig. 7. The self-consistent mass-ratio m_ρ/m_π and coupling γ as functions of the cut-off Λ. As always, the case (a) corresponds to absence of short-range force and the case (b) to presence of short-range force. Experimental values: $(m_\rho/m_\pi)^2 = 30$, $\gamma = 3.8$.

Fig. 8. Appropriate mapping (defined by (B.1)) of the resolvent of Eq. (A.8), which determines its structure in λ.

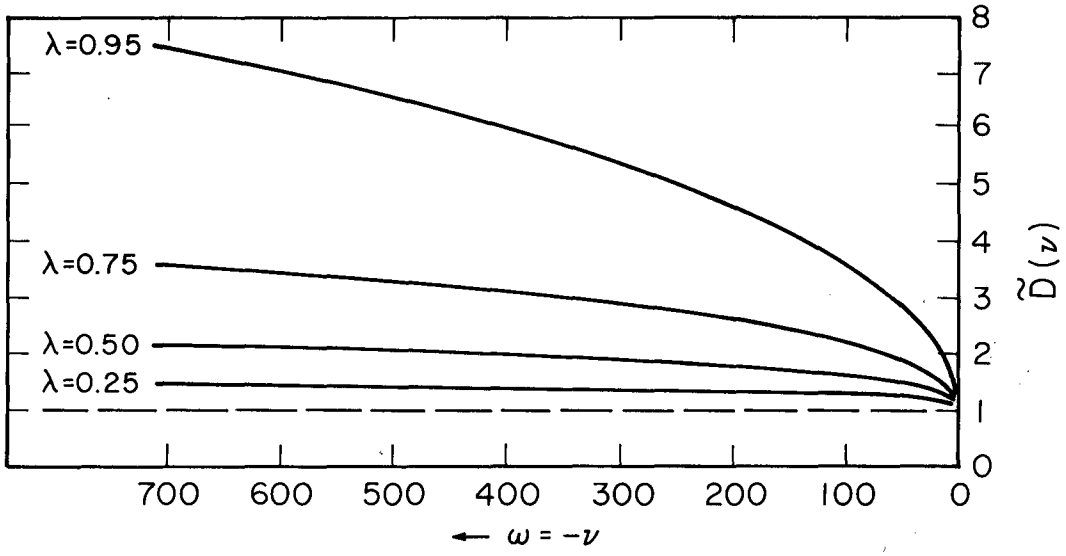

XBL672-757

Fig. 1

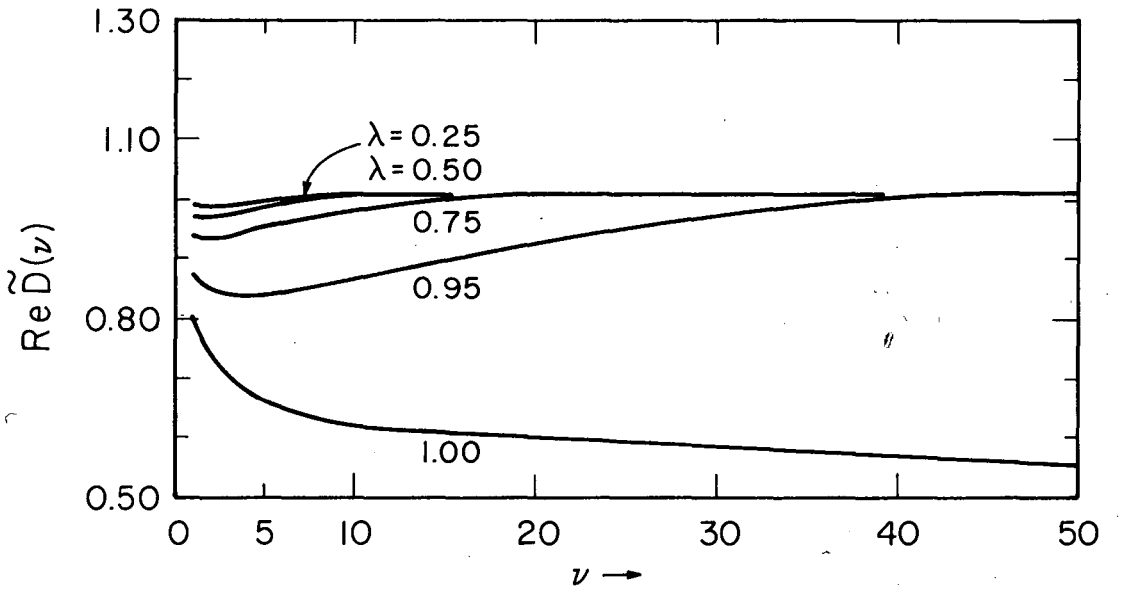

XBL672-758

Fig. 2

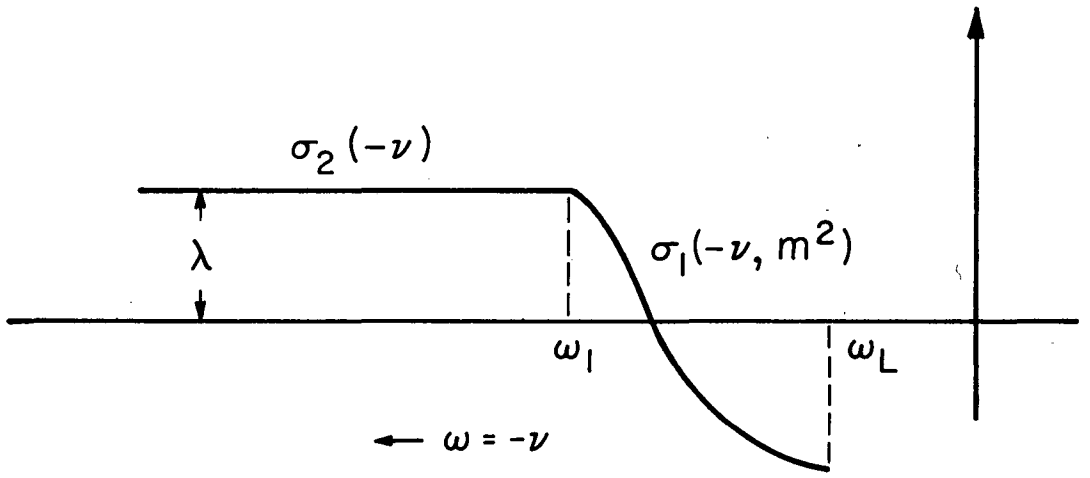

XBL672-759

Fig. 3

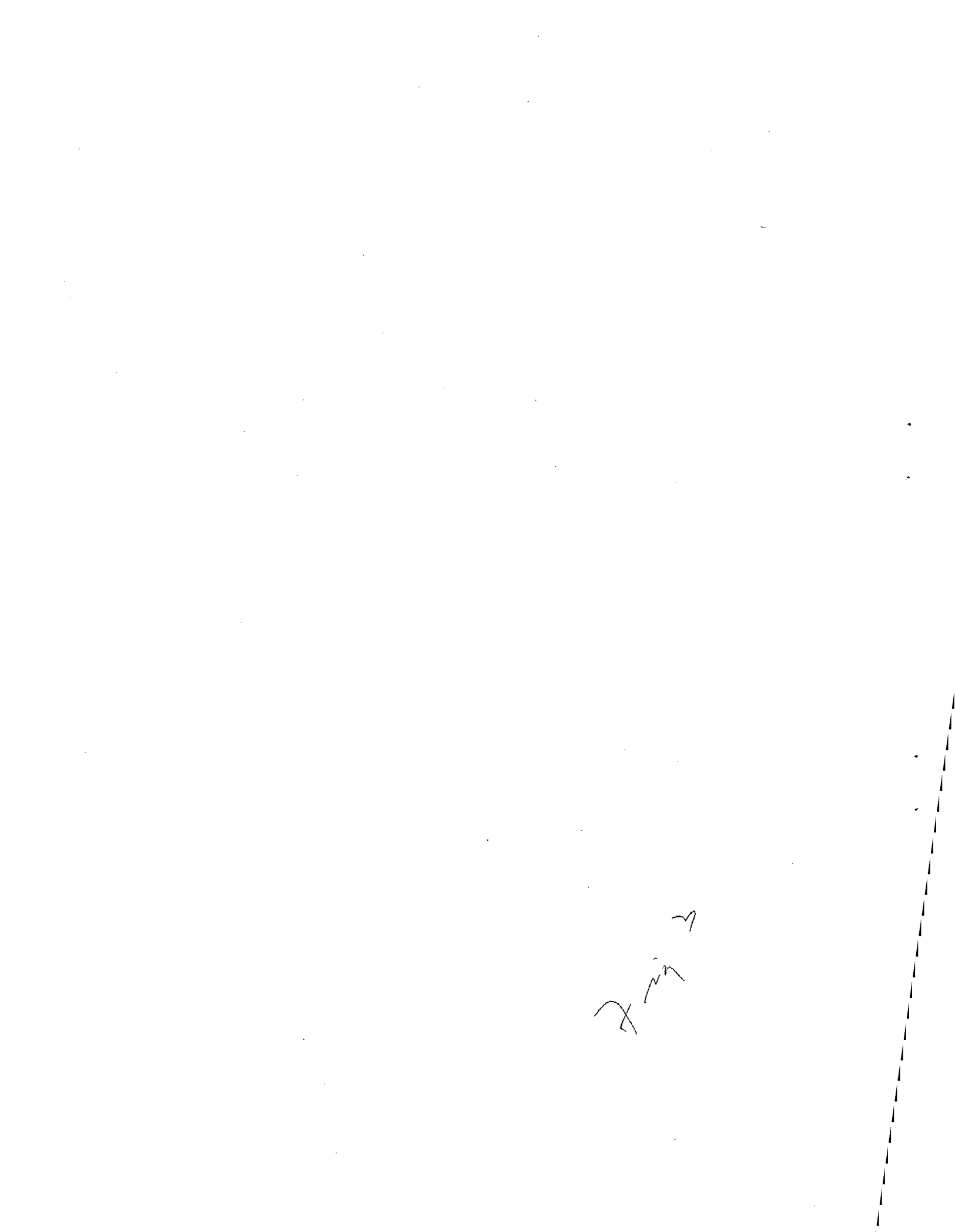

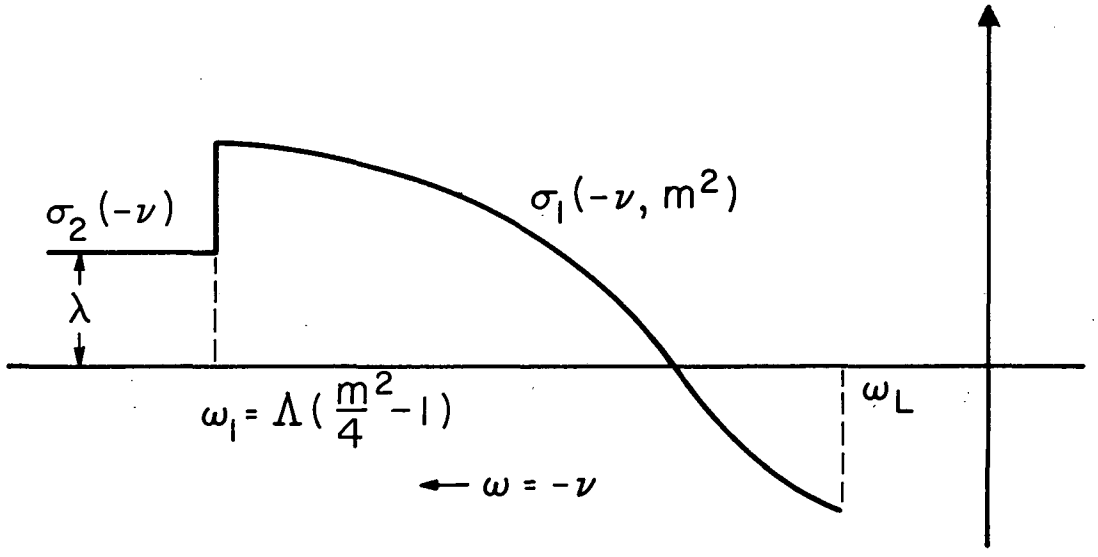

XBL672-760

Fig. 4

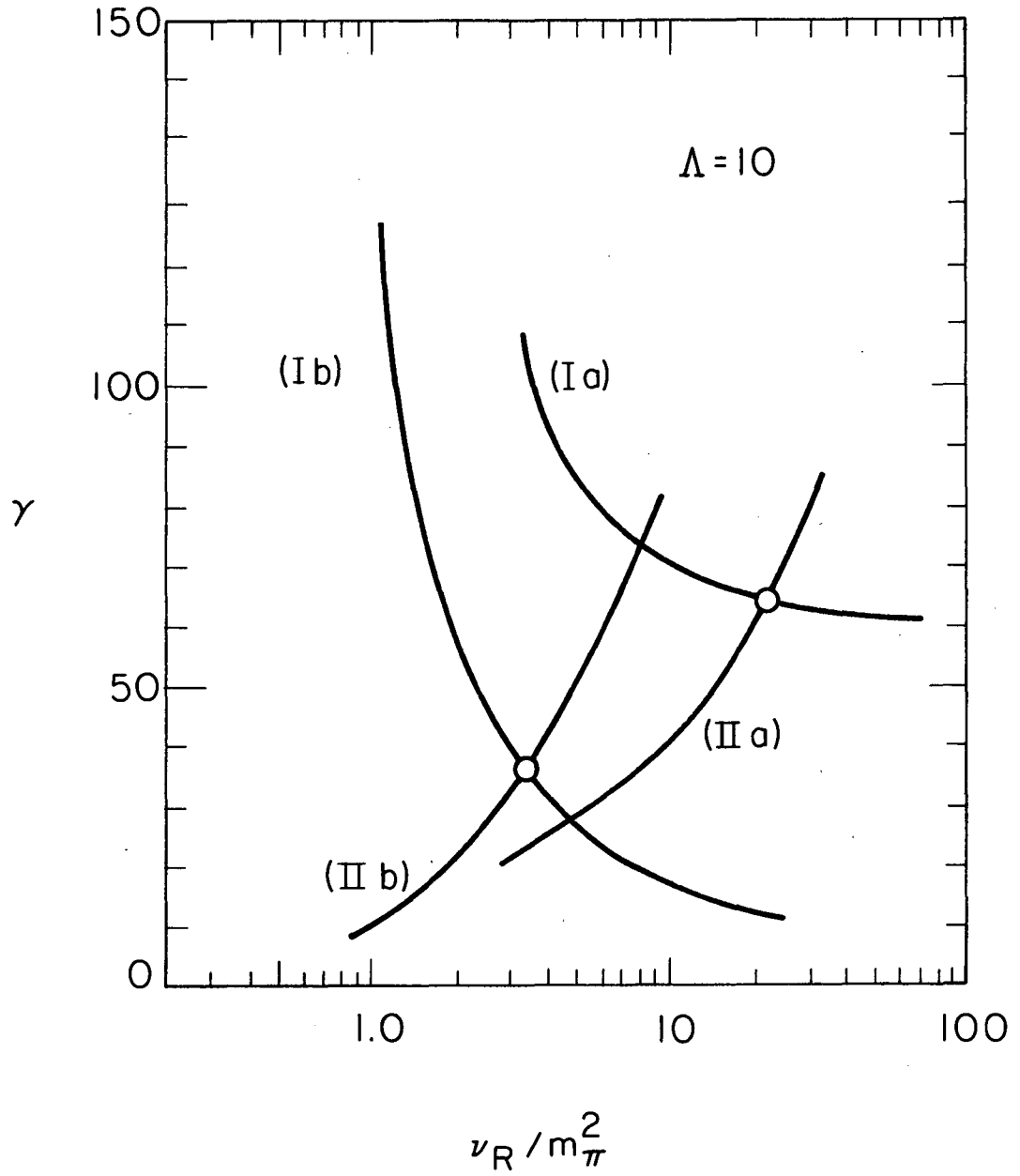

XBL 672-761

Fig. 5

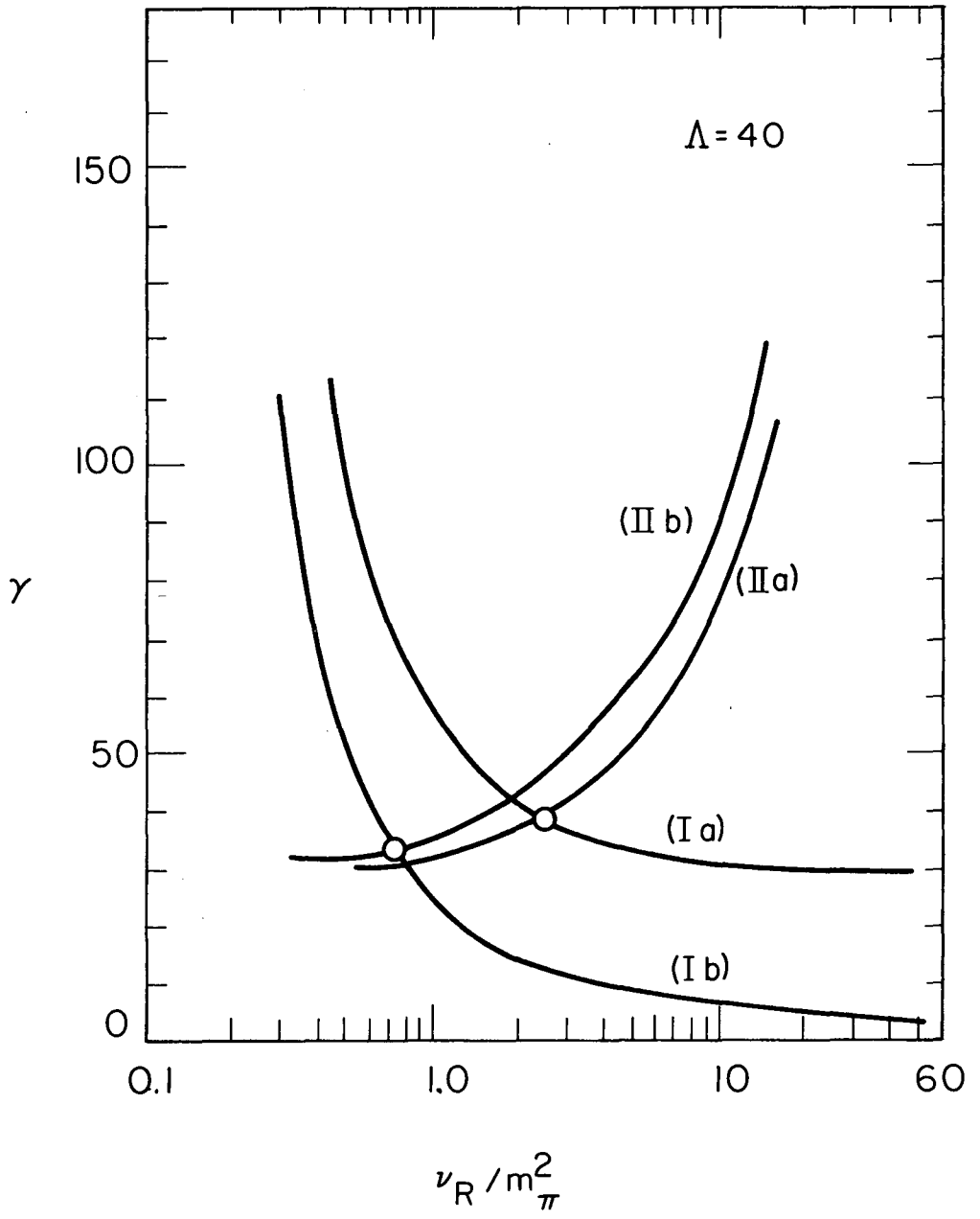

XBL672-762

Fig. 6

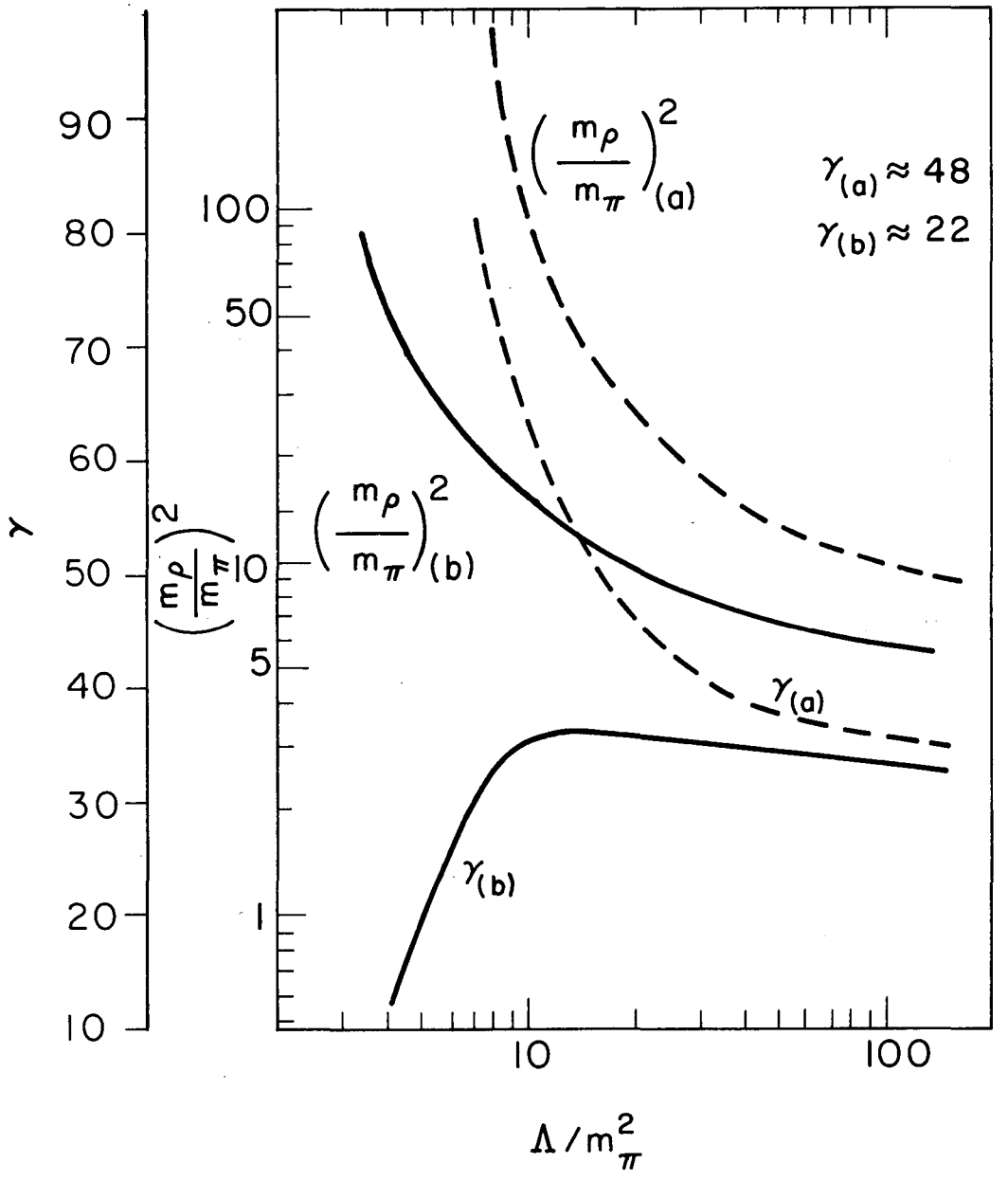

XBL 672-763

Fig. 7

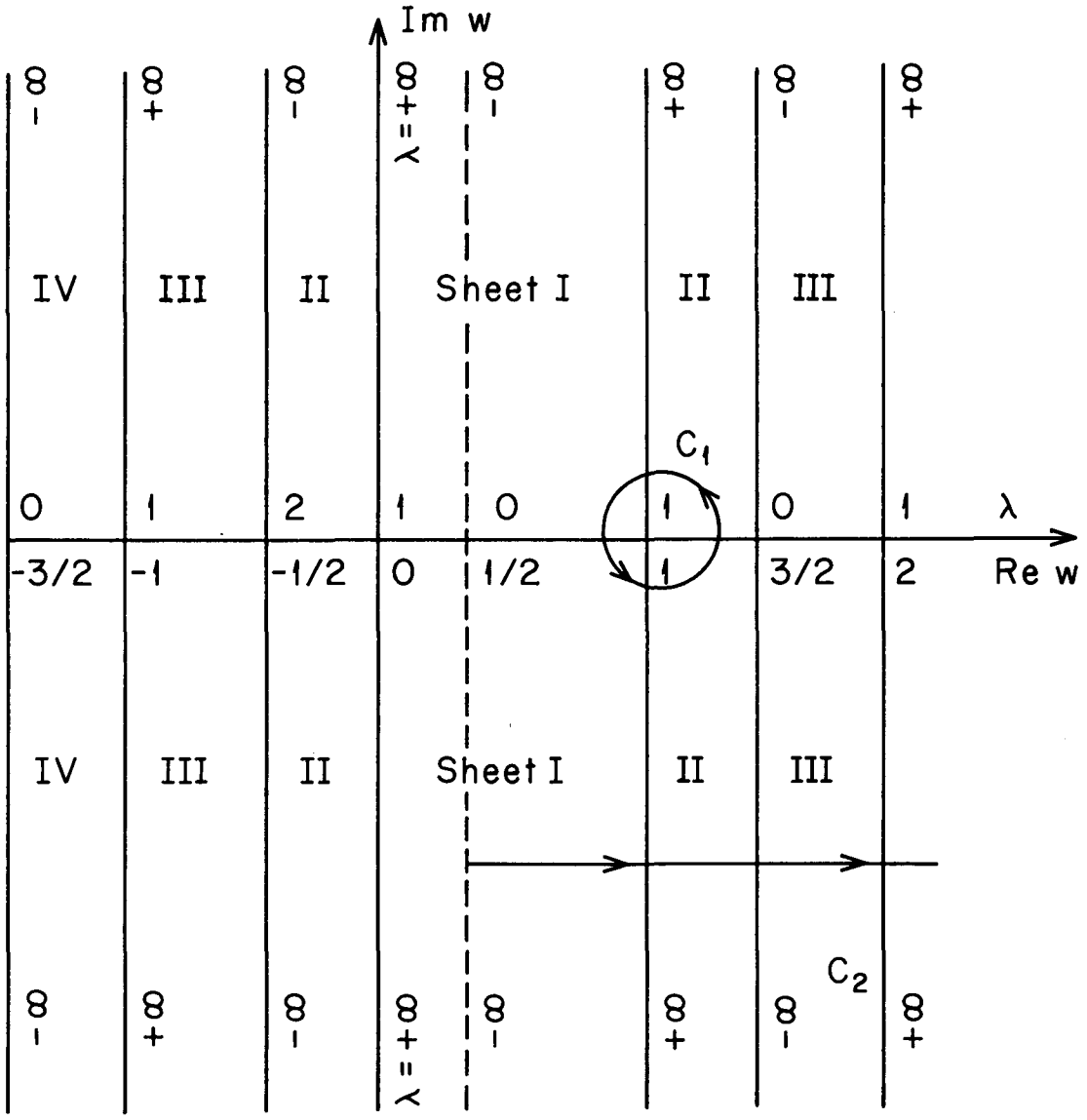

XBL674-2210

Fig. 8